

# Matter Power Spectrum from the Lyman- $\alpha$ Forest: Myth or Reality?

Nikolay Y. Gnedin<sup>1</sup> and Andrew J. S. Hamilton<sup>2</sup>

<sup>1</sup>Center for Astrophysics and Space Astronomy, University of Colorado, Boulder, CO 80309; gnedin@casa.colorado.edu

<sup>2</sup>JILA, University of Colorado, Boulder, CO 80309; Andrew.Hamilton@colorado.edu

8 March 2022

## ABSTRACT

We investigate possible systematic errors in the recent measurement of the matter power spectrum from the Lyman- $\alpha$  forest by Croft et al. (2001). We find that for a large set of prior cosmological models the Croft et al. result holds quite well, with systematic errors being comparable to random ones, when a dependence of the recovered matter power spectrum on the cosmological parameters at  $z \approx 3$  is taken into account. We find that peculiar velocities cause the flux power spectrum to be smoothed over about 100–300 km/s, depending on scale. Consequently, the recovered matter power spectrum is a smoothed version of the underlying true power spectrum. Uncertainties in the recovered power spectrum are thus correlated over about 100–300 km/s.

As a side effect, we find that residual fluctuations in the ionizing background, while having almost no effect on the recovered matter power spectrum, significantly bias estimates of the baryon density from the Lyman- $\alpha$  forest data.

We therefore conclude that the Croft et al. result provides a powerful new constraint on cosmological parameters and models of structure formation.

**Key words:** cosmology: theory – cosmology: large-scale structure of universe – galaxies: formation – galaxies: intergalactic medium

## 1 INTRODUCTION

The Lyman- $\alpha$  forest is perceived as being simple, and in this simplicity promises to become a key to many unsolved problems in cosmology. In the most recent demonstration of the power of simplicity, Croft et al. (2001) presented a measurement of the matter linear power spectrum on scales which are nonlinear today – a measurement not easily reproducible by other means, such as galaxy surveys at low redshift.

Not only was the phenomenon that they modeled simple, but also the method that they used to recover the linear power spectrum was simple – perhaps excessively simple. For example, Croft et al. (2001) considered only one prior cosmological model in deriving the correction function that translates the observed flux power spectrum into a linear power spectrum.

In this paper our purpose is to check whether their method is reliable by sampling over a range of prior cosmological models. We also attempt to estimate systematic errors and their covariance. We begin in §2 by making sure that we are able to reproduce Croft et al. (2001) results. In §3 we give our results. We close in §4 with an optimistic conclusion.

## 2 METHOD

Since our goal is to evaluate the accuracy of the Croft et al. (2001) method, we apply their method to a range of cosmological models. We adopt the same linear transfer function, but we vary the amplitude and the tilt, and we experiment with different geometries and different Hubble constants. In §3.2 we also report the effect of varying the linear power spectrum over narrow intervals of wavenumber. We use a standard Particle-Mesh method to simulate the distribution of the matter at  $z = 2.72$ . Following Croft et al. (2001) we assume that the underlying baryon density follows that of the dark matter. At small scales the baryon density is smoothed out compared to the dark matter density, but the scale at which this occurs, the “filtering” scale, is much smaller than the range of scales of interest here (Gnedin & Hui 1998) (we discuss this in detail in §3.3.2). All our simulations have a box size of  $20h^{-1} \text{ Mpc}$  (in comoving coordinates) and  $256^3$  particles on a mesh of the same size. The gravitational force is calculated with a Green function that includes the Optimal Antialiasing Filter (Ferrell & Bertschinger 1994), by summing over three Brillouin zones.

In calculating the synthetic Lyman- $\alpha$  absorption spectra we follow the Croft et al. (2001) procedure in

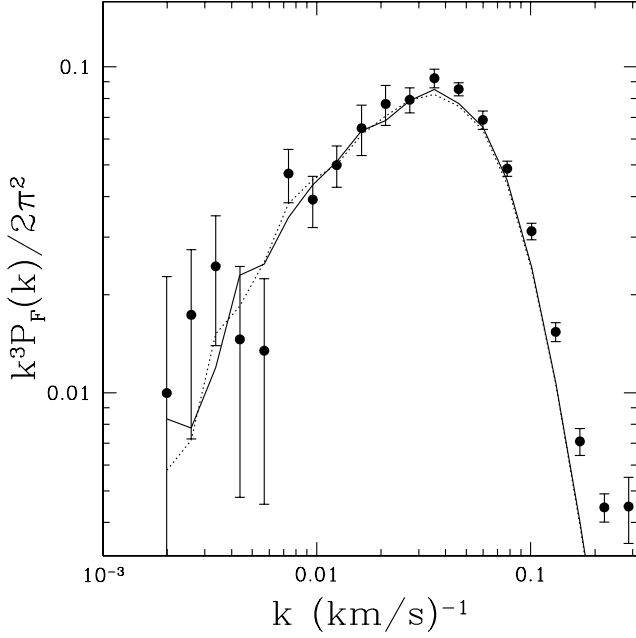


Figure 1. The  $\text{ux}$  power spectrum predicted by the Croft et al. (2001) dual model, compared to the observed  $\text{ux}$  power spectrum from Croft et al. (2001). The dotted line is the model averaged over 3 best realizations (roughly equivalent to 100 random realizations) while the solid line is averaged over 12 best realizations (roughly equivalent to 400 random realizations).

precise detail: we compute the synthetic spectra for 1000 lines of sight which cross the computational box at random angles (to avoid bias introduced for lines of sight parallel to the box sides) for an assumed value for the spatial homogeneous photoionization rate. We then compute the mean opacity ( $\bar{\tau}$ ) and find the value of  $\tau$  that gives the desired value for the mean opacity ( $\bar{\tau} = 0.349$  except as described in x3.1.3). We then compute the 1D  $\text{ux}$  power spectrum of the normalized  $\text{ux}$  for each line of sight using a Lomb periodogram and average the results over 1000 lines of sight. We have verified that this number (1000 lines of sight) is fully sufficient to obtain numerical results with the precision well below the observational error.

Before we can test for systematic errors in the Croft et al. (2001) method, we must first check that we can reproduce their results accurately.

In order to reduce the uncertainty in the mean  $\text{ux}$  power spectrum, an average of several different random realizations is usually used. Normally, this procedure requires a large number of realizations, because the variance decreases only as the square root of the number of realizations. Instead, we adopt a slightly different approach. Out of all random realizations, we first choose “good” ones, i.e. those that give a measured linear power spectrum close to the input linear power spectrum. We choose 3 “best” realizations out of 100 random ones, and an average over those three recovers the input power spectrum at least as well as a plain average over 100 truly random realizations.

Figure 1 shows the  $\text{ux}$  power spectrum  $P_F(k)$  (shown as  $k^3 P_F(k) / (2\pi^2)$ ) averaged over 3 and over 12 best realizations (equivalent of 100 and 400 random realizations). The difference between the two curves provides an estimate

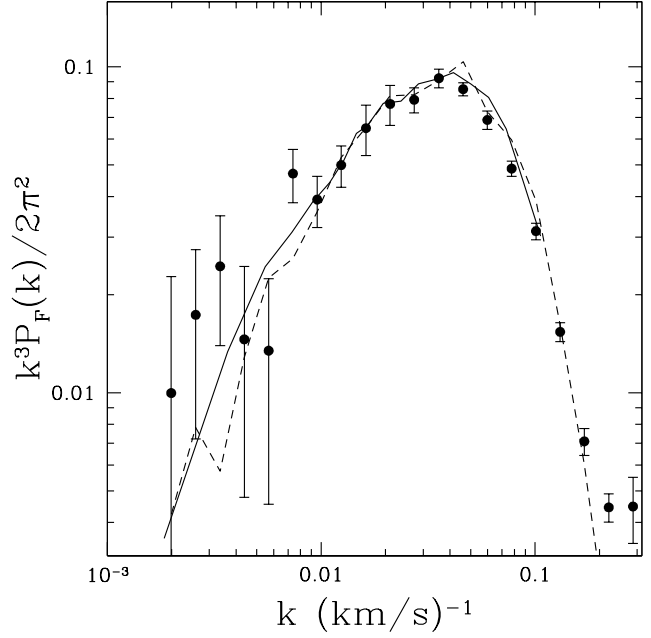


Figure 2. The  $\text{ux}$  power spectrum from the Croft et al. (2001) dual model (solid line) and our reproduction of their result (dashed line).

of about 1/2 of the uncertainty in the mean  $\text{ux}$  power spectrum (because averaging over 12 realizations gives half the variance of averaging over just 3 realizations). We notice that this difference is significantly smaller than the statistical error bars of the observational data, indicating that our  $\text{ux}$  power spectrum is calculated with sufficient precision.

Hereafter we use three “good” realizations per normalization for each cosmological model. Thus, each model requires at least six simulations (two different normalizations above and below the best-fit value), and more if our initial choice for the two normalizations does not bracket the best-fit value.

As evidence that our method reproduces the Croft et al. (2001) results, we show in Figure 2 their dual model (courtesy Rupert Croft) and the  $\text{ux}$  power spectrum from our simulation of exactly the same cosmological model. Notice that there exist a difference on large scales, which is most likely due to the smaller size of our computational box, but that it is smaller than the observational errors and so is unimportant.

### 3 RESULTS

#### 3.1 Systematic errors of the recovered linear power spectrum

In this paper our main concern is the effect that an assumption of a specific cosmological model makes on recovering the linear power spectrum from the  $\text{ux}$  power spectrum. Specifically, Croft et al. (2001) assume that the  $\text{ux}$  power spectrum  $P_F(k)$  is proportional to the linear power spectrum  $P_L(k)$  at the same wavenumber

$$P_F(k) = b^2(k) P_L(k) \quad (1)$$

the bias factor  $b(k)$  being independent of, or at least insensitive to, the power spectrum  $P_L(k)$ .

If the "bias factor"  $b(k)$  were independent of the linear power spectrum, this would be a direct analogy to the biased galaxy linear power spectrum. However, this is not the case – the "bias factor"  $b(k)$  depends on the amplitude of the linear power spectrum  $P_L(k)$ , so that the relation (1) is not a linear relation. Correctly, equation (1) should be written as

$$P_F(k) = b^2[k; P_L] P_L(k); \quad (2)$$

where we use the square brackets to underline that  $b$  is actually an operator acting on the linear power spectrum  $P_L(k)$ . Thus, the recovered "observed" linear power spectrum,

$$P_L^{\text{obs}}(k) = \frac{P_F^{\text{obs}}(k)}{b^2[k; P_L]}; \quad (3)$$

actually depends on the assumed linear power spectrum, and this dependence appears as a systematic error which is not included in the estimate of the error bars by Croft et al. (2001).

For a particular choice of  $P_L$  that fits the observed flux power spectrum, relationship (2) can be linearized. For small deviations  $\delta P_L$  about an assumed linear power spectrum  $P_L$ , we obtain

$$P_F(k) = \sum_{k^0} b^2(k; k^0) P_L(k^0); \quad (4)$$

where the matrix  $b(k; k^0)$  can be obtained by differentiating equation (2). Even in this linearized form this equation is more complicated than the Croft et al. (2001) assumption (1).

Throughout this paper, when we refer to the "recovered linear power spectrum", we always mean  $P_L^{\text{obs}}(k)$  obtained via equation (3). The sole purpose of this paper is to investigate how the dependence of  $b$  on  $P_L$ , ignored by Croft et al. (2001), affects the recovery procedure.

### 3.1.1 Dependence on the Hubble constant or spectral curvature

An important part of the Croft et al. (2001) procedure is the translation from the spatial units used in a simulation to velocity units of the observational data. This requires adopting a value for the Hubble constant at  $z = 2.72$  which is used to scale spatial scales to velocity space. Specifically, following Croft et al. (2001), we adopt

$$v_{\text{tot},i} = H_3 (r_i + v_{\text{pec},i}/H_{\text{EdS},3}); \quad (5)$$

where  $r_i$  is the physical position of a pixel  $i$  in the synthetic spectrum,  $v_{\text{tot},i}$  is the velocity position of the same pixel,  $v_{\text{pec},i}$  is the peculiar velocity of a given pixel in the simulation (in the EdS cosmology),  $H_3$  is the adopted value of the Hubble constant at  $z = 2.72$ , and  $H_{\text{EdS},3} = 720 h \text{ km/s/Mpc}$  is the Hubble constant in the EdS cosmology at  $z = 2.72$ . This procedure is identical to the one adopted in Croft et al. (2001): we have applied our procedure to the simulation data kindly provided to us by Rupert Croft, and we obtained numerically indistinguishable results.

It is important to emphasize here that this rescaling of the Hubble constant only affects the transformation from position to velocity space. The primordial power spectrum

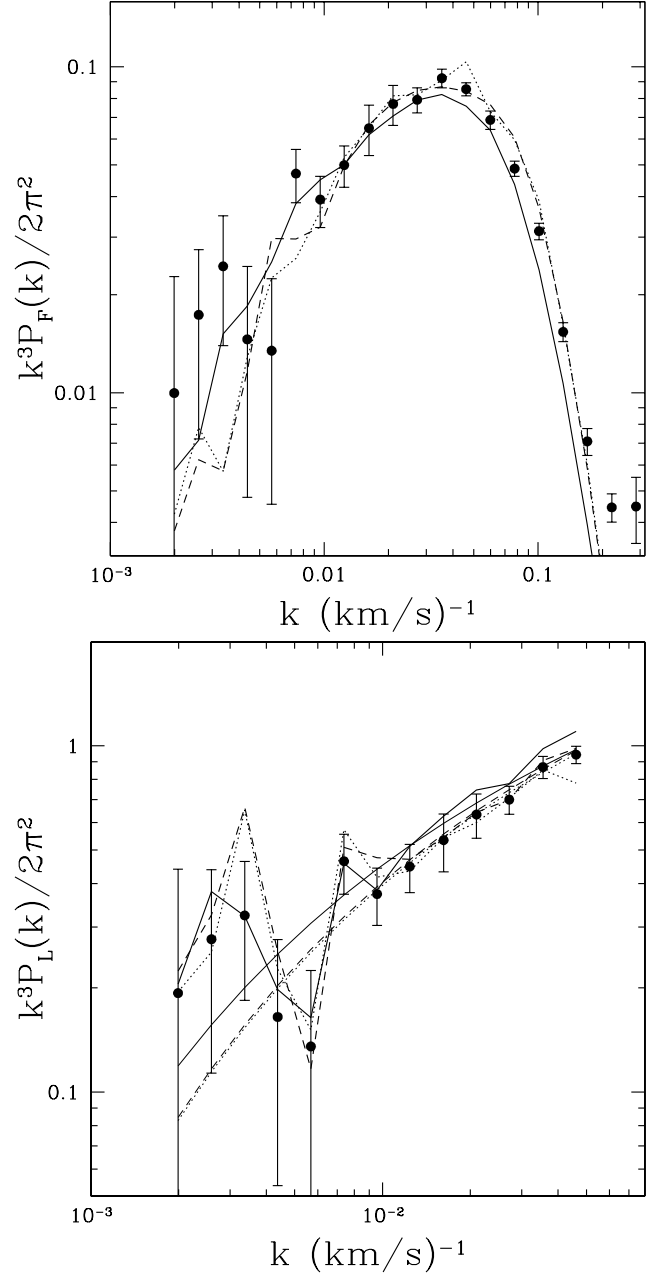


Figure 3. (a) The flux power spectrum and (b) the recovered linear power spectrum  $P_L^{\text{obs}}$  in the Croft et al. (2001) fiducial model (EdS cosmology; solid line), the same cosmological model with the Hubble constant rescaled to a value appropriate to a flat cosmology with  $\Omega_m = 0.4$  (just like in Croft et al.; dotted line), and for the flat cosmological model with  $\Omega_m = 0.4$  (dashed line). Thin solid lines in this and all following figures show the assumed linear power spectrum  $P_L$  for the underlying cosmological model.

of fluctuations as a function of position adopted in the simulations is not changed, but rescaling of the velocity units does result in the linear power spectra being different in velocity space.

It can be shown that for pure power-law power spectra all the dependence on the Hubble constant cancels out exactly. However, this is not true for a general power spectrum with varying slope. In order to test this dependence

we have run a low density at cosmological model in addition to the fiducial model. Both models have identical initial conditions, and both run in the matter-dominated universe ( $\Omega_m = 1$  for both models). They differ only by the values of the Hubble constant  $H = H_0 \Omega_m^{-1/2} (1+z)^{3/2}$ , which are different by a factor  $\Omega_m^{-1/2} = 0.6$ . Croft et al. (2001) did not use a Hubble constant appropriate to their cosmological model. Rather, they ran the simulation in the EdS cosmology, but adopted the Hubble constant from a flat cosmology with  $\Omega_m = 0.4$ . We also show the so rescaled model in Fig. 3 (which is the model also shown in Fig. 2). As can be seen from Figure 3, the three recovered power spectra differ by less than the random error of the measurement, and we thus conclude that the dependence on the Hubble constant (or, equivalently, on the rate of change in the local slope – but see §3.2) is insignificant.

### 3.1.2 Assumed effective equation of state

Croft et al. (2001) point out that uncertainty in the effective equation of state of the IGM, i.e. in the relationship between the temperature and the density of the photoionized gas, is one of the dominant systematic errors in recovering the linear power spectrum. This relation is commonly parameterized as (Hui & Gnedin 1998)

$$T = T_0 (1 + \delta)^{\beta}; \quad (6)$$

where  $T_0$  and  $\beta$  are parameters and  $\delta$  is the gas overdensity. Croft et al. (2001) adopt the values of  $T_0 = 15,000$  K and  $\beta = 1.6$ . However, recent measurements of the effective equation of state at  $z = 3$  (Ricotti et al. 2000; Schaye et al. 2000; McDonald et al. 2001) suggest somewhat different values for these parameters:  $T_0 = 20,000$ – $3,000$  K and  $\beta = 1.3$ – $0.2$  at  $z = 2.72$  (all three measurements taken together and weighted by their uncertainties). We have run the six models with values for  $T_0$  and  $\beta$  in the observed range, and the results are shown in Figure 4. We find that the effect of the slope  $\beta$  on the recovered power spectrum is small, below the random uncertainties of the measurement, and so we do not attempt to model it, but regard it as part of the total systematic error quoted in Table 1. The amplitude  $T_0$  however does affect the recovered linear power spectrum, which scales approximately inversely proportionally to  $T_0$ ,

$$P_L(k; T_0) = P_L(k; 20,000 \text{ K}) \frac{20,000 \text{ K}}{T_0}; \quad (7)$$

Rescaling the recovered power spectra this way reduces the rms difference between various models to about 1%.

This dependence is easy to understand: for a given density and velocity distribution and a given photoionization rate, higher temperature means broader absorption lines, which in turn implies a lower mean opacity. When the mean opacity is renormalized to the fiducial value 0.349, the photoionization rate is adjusted downward, and a given value of the flux now corresponds to a lower value of the density and thus the lower amplitude of the power spectrum (since readjustment of the photoionization rate scales all densities by the same factor).

Because the value  $T_0 = 20,000$  K is favored by observations, we adopt this value as our fiducial value in the rest of this paper.

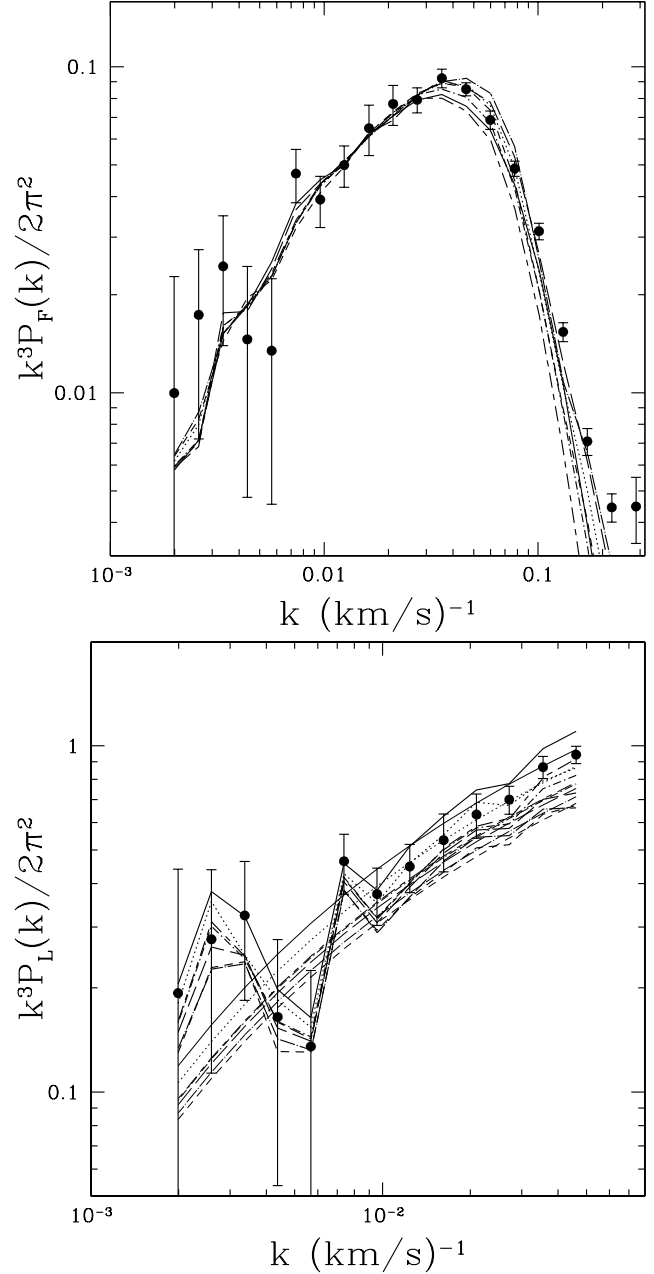


Figure 4. The flux power spectrum (a) and the recovered linear power spectrum (b) in the Croft et al. (2001) model with different assumed effective equations of state:  $T_0 = 15,000$  K,  $\beta = 1.6$  (solid line, Croft et al. assumed values),  $T_0 = 20,000$  K,  $\beta = 1.2$  (dotted line),  $T_0 = 23,000$  K,  $\beta = 1.2$  (short-dashed line),  $T_0 = 17,000$  K,  $\beta = 1.2$  (long-dashed line),  $T_0 = 20,000$  K,  $\beta = 1.4$  (dot { short-dashed line), and  $T_0 = 20,000$  K,  $\beta = 0.9$  (dot { long-dashed line).  $T_0 = 20,000$  K,  $\beta = 1.6$  (short-dashed { long-dashed line).

### 3.1.3 Assumed mean optical depth

Another possible systematic error discussed by Croft et al. (2001) is the assumed value for the mean optical depth – the value used to normalize synthetic absorption spectra. They assumed a value of  $\tau = 0.349$  based on Press, Rybicki, & Schneider (1993) (hereafter PRS) value. The PRS measurement actually gives  $\tau_{\text{PRS}} = 0.349^{+0.051}_{-0.034}$ . A more recent measurement by McDonald et al. (McDonald

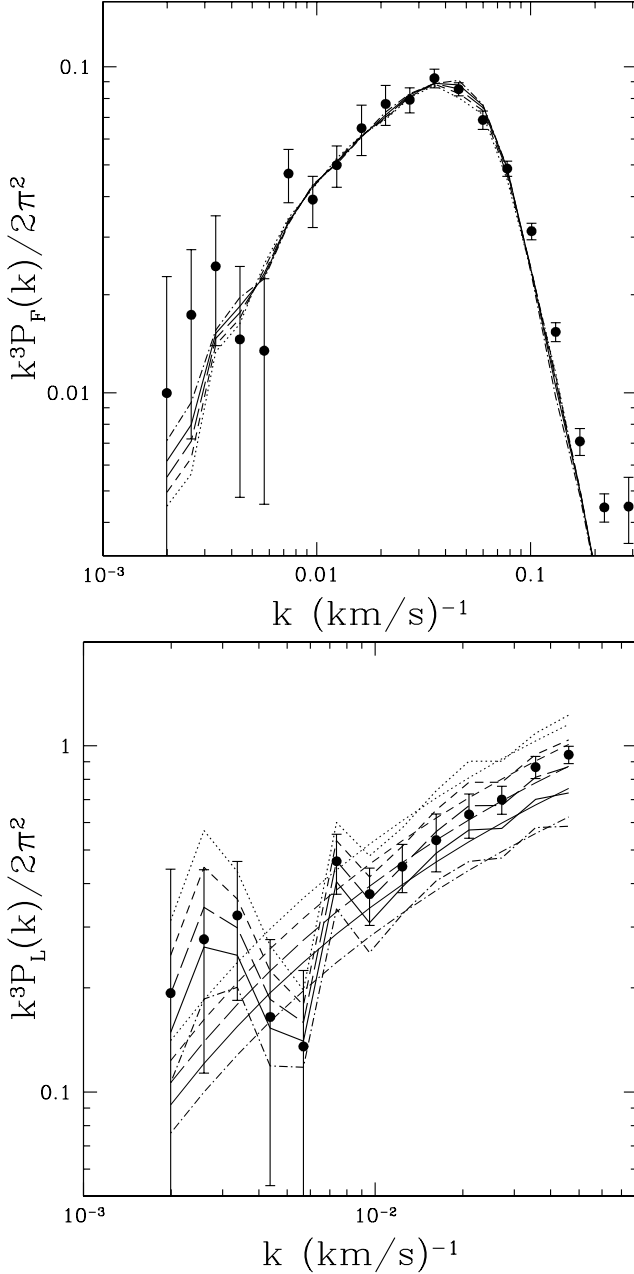


Figure 5. The flux power spectrum (a) and the recovered linear power spectrum (b) in the Croft et al. model with different assumed values for the mean optical depth:  $\bar{\tau} = 0.349$  (solid line, Croft et al. assumed value),  $\bar{\tau} = 0.260$  (dotted line),  $\bar{\tau} = 0.285$  (short-dashed line),  $\bar{\tau} = 0.315$  (long-dashed line),  $\bar{\tau} = 0.400$  (dot-dashed line).

et al. 2000) (hereafter MCD) gives a somewhat lower value,  $\bar{\tau}_{MCD} = 0.285 \pm 0.025$ . In order to test all the parameter range suggested by observations, we have run four models with the mean optical depth different from the fiducial value:  $\bar{\tau} = 0.400$  (PRG+1),  $\bar{\tau} = 0.315$  (PRG-1 and about MCD+1),  $\bar{\tau} = 0.285$  (MCD value), and  $\bar{\tau} = 0.260$  (MCD-1). The flux power spectra and the recovered linear power spectra for these four cases and the fiducial case are given in Figure 5. As one can see, the recovered power spectra scale with  $\bar{\tau}$ . We find a somewhat weaker dependence than

that reported by Croft et al. (2001), mostly because we only consider a range of optical depth around the observed values. The following simple power-law scaling takes out almost all dependence of the recovered linear power spectrum on  $\bar{\tau}$  (the rms difference between the rescaled power spectra is less than 1%):

$$P_L(k; \bar{\tau}) = P_L(k; 0.349) \frac{0.349}{\bar{\tau}}^{0.75} \quad (8)$$

The physical origin of this dependence is also clear: lower  $\bar{\tau}$  means higher densities for the same value of the flux.

### 3.1.4 Slope of the prior power spectrum

Another possible source of systematic error is the slope of the prior linear power spectrum  $P_L(k)$ . We test four models, with  $n = 1.0$ ,  $n = 0.95$  (the Croft et al. model),  $n = 0.9$ , and  $n = 0.7$ . Figure 6 shows the flux and recovered linear variance for these models. The  $n = 0.7$  model does not fit the flux power spectrum as well as other models, but the fit is still statistically acceptable ( $\chi^2 = 11$  with 11 degrees of freedom). In all cases however, the recovered linear power spectrum agrees well with the fiducial model, indicating that the method is insensitive to quite significant variations in the slope of the prior power spectrum. In other words, the effective bias factor  $b(k)$  in equation (1) appears similar for all the model spectra, an encouraging result.

### 3.1.5 Dependence on the matter density

Similarly, the dependence on the matter density parameter at  $z = 2.72$ ,  $\Omega_{m,3}$ , was not tested by Croft et al. (2001). This may not be an issue after all, because for any reasonable fiducial model with a cosmological constant,  $\Omega_{m,3} = 1$  to better than 5%. Nevertheless, we have tested the matter density dependence. We have run three open models with  $n = 0.7$  and  $\Omega_{m,0} = 0.45$  ( $\Omega_{m,3} = 0.75$ ),  $\Omega_{m,0} = 0.2$  ( $\Omega_{m,3} = 0.5$ ), and  $\Omega_{m,0} = 0.1$  ( $\Omega_{m,3} = 0.3$ ) respectively, and the results of these simulations are presented in Figure 7. One can see that the recovered linear power spectrum does depend on the assumed value of the density parameter at  $z = 2.72$ , even if all three models fit the observed flux power spectrum.

The dependence on the density parameter cannot be rigorously derived analytically, but the form found empirically can be understood approximately on the basis of arguments from linear theory. The Gunn-Peterson optical depth

(Gunn & Peterson 1965) at every spatial point is inversely proportional to the  $du/dx$  along the line of sight (Hu et al. 1997), where  $u$  is the total velocity (Hubble flow plus peculiar velocity) and  $x$  is the comoving distance. In the linear regime

$$\frac{du}{dx} = \frac{\partial u}{\partial x} = aH(1+f); \quad (9)$$

where  $f = d \ln D / d \ln a = 0.6$ . The first term in the parenthesis is the Hubble flow, while the second one is due to peculiar velocities. In the linear regime the Hubble flow of course dominates, but at  $z = 3$  most of the Lyman- $\alpha$  forest is mildly nonlinear, with  $k^3 P_L(k) = (2/2)^{-1}$ , as can be seen from Fig. 7.

If we assume that different  $k$  values are independent

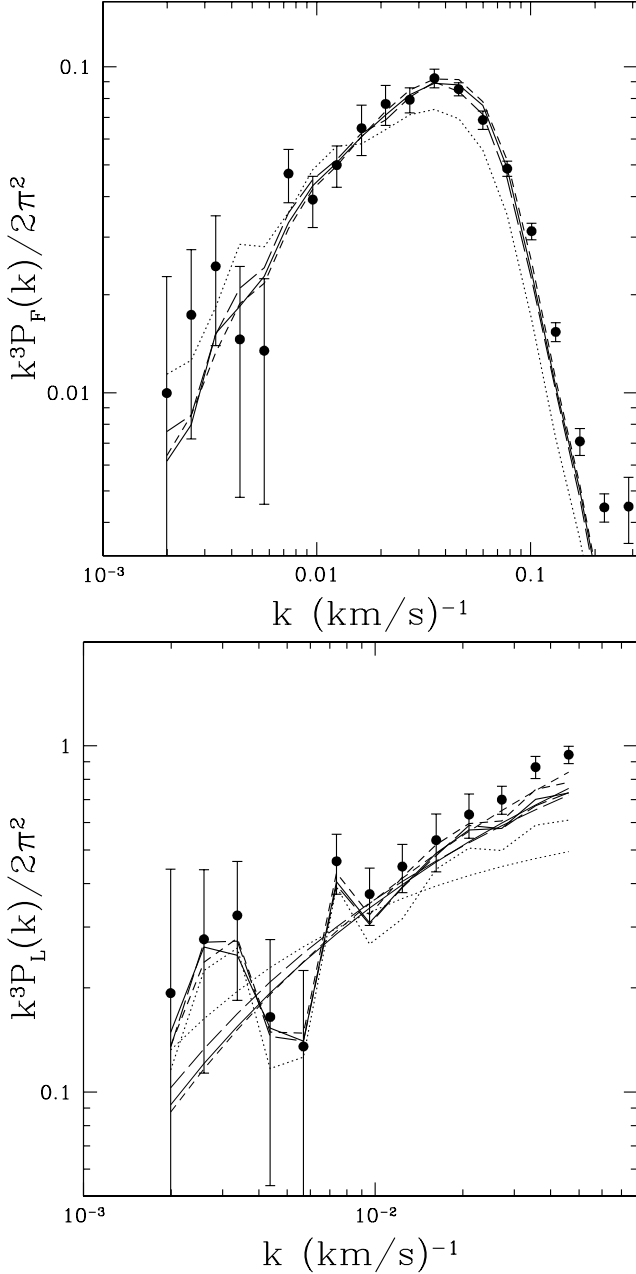


Figure 6. The flux power spectra (a) and the recovered linear power spectra (b) in four cosmological models with the different slope of the primordial power spectrum, as shown by thick lines:  $n = 0.95$  (solid line, Croft et al. fiducial model), the same model with  $n = 0.9$  (long-dashed line),  $n = 1.0$  (short-dashed line), and  $n = 0.7$  (dotted line). Thin lines in panel (b) show the prior linear power spectra for these models and symbols show the data from Croft et al. (2001).

(which is not quite true, but good enough for our hand-waving arguments), we would expect that the power spectrum for the optical depth is approximately inversely proportional to  $(1 + f_k)^2$ . In other words, we hypothesize that the recovered linear power spectrum depends on cosmological parameters in the following way:

$$P_L^{\text{obs}}(k) = P_L^{\text{fct}}(k) \frac{1 + \frac{k}{f_3}}{1 + f_3 k}^2; \quad (10)$$

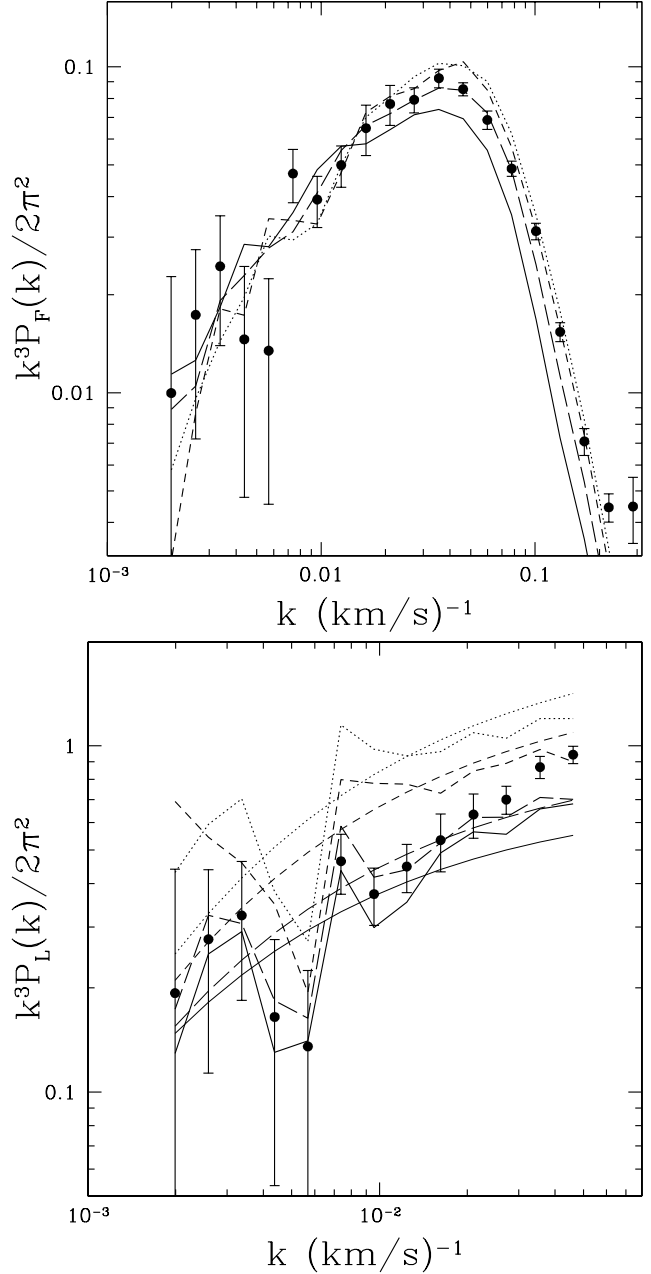


Figure 7. The flux power spectrum (a) and the recovered linear power spectrum (b) in four different cosmological models: Croft et al. (2001) fiducial model (solid line), an open model with  $\Omega_m = 0.45$  and  $n = 0.7$  (long-dashed line), an open model with  $\Omega_m = 0.2$  and  $n = 0.7$  (long-dashed line), and an open model with  $\Omega_m = 0.1$  and  $n = 0.7$  (dotted line).

where we will call  $P_L^{\text{fct}}(k)$  the "factorized" linear power spectrum,  $f_3$  is the value of  $f$  at  $z = 2.72$ , and

$$k \frac{k^3 P_L^{\text{obs}}(k)}{2 \pi^2}^{1/2} \quad (11)$$

and thus depends on  $P_L^{\text{obs}}(k)$ . In this form  $P_L^{\text{fct}}(k)$  should be nearly independent of the value of the matter density parameter at  $z = 2.72$ .

Figure 8 now gives  $P_L^{\text{fct}}(k)$  for the four models shown in 7. As one can see, the factorization (10) does account for the

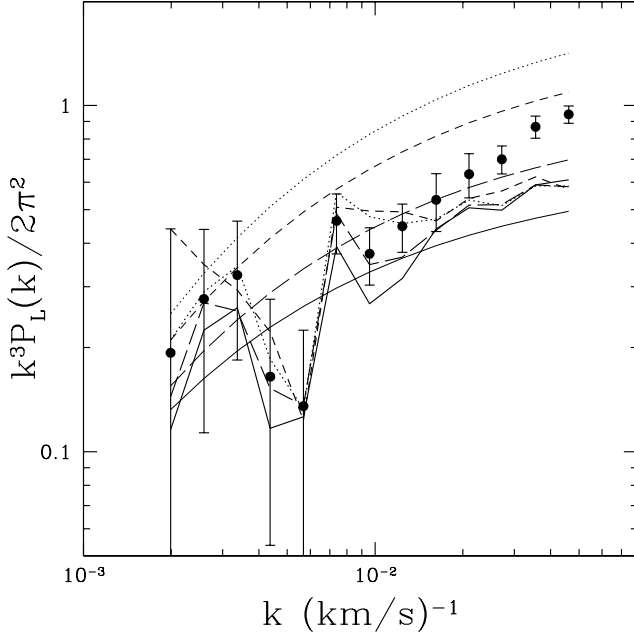


Figure 8. The factorized recovered linear power spectrum in four cosmological models from Fig. 7. Line markings are the same.

main dependence of the recovered linear power spectrum on cosmological parameters, although some differences remain. It is however not convenient to use in practice because it is nonlinear and implicit for  $P_L^{\text{obs}}(k)$ . But we can notice that for  $m_{\text{gas}}$  substantially different from 1,  $k_{\text{gas}}$  is about unity for the range of scales where the observational error-bars are small. It turns out that a comparable factorization can be obtained if we adopt a fixed value  $k_{\text{gas}} = 1.4$  in equation (10),

$$P_L^{\text{obs}}(k) = P_L^{\text{fct}}(k) \frac{2.4}{1 + 1.4f_3} \quad (12)$$

This is linear, so it is easier to use in joint parameter estimation, while it still recovers the density dependence to about 2.2% precision.

### 3.1.6 The systematic error of the recovered linear power spectrum

We can now summarize our results. The recovered linear power spectrum can be factorized in the following way:

$$P_L^{\text{obs}}(k) = P_L^{\text{fct}}(k) Q_{\text{T}} Q_{\text{S}} \quad (13)$$

where

$$Q_{\text{S}} = \frac{2.4}{1 + 1.4f_3} \quad (14)$$

$$Q_{\text{T}} = 20,000 \text{ K} = T_0;$$

$$Q_{\text{D}} = (0.349)^{0.75};$$

and  $P_L^{\text{fct}}(k)$  is independent of anything else (just numbers) and is shown in Figure 9 and in Table 1 together with its "systematic" error-bars. We put the word "systematic" in quotes because we considered only a subsample of all possible cosmological models, and our sampling of the parameter space is by no means uniform. We thus suggest that errors

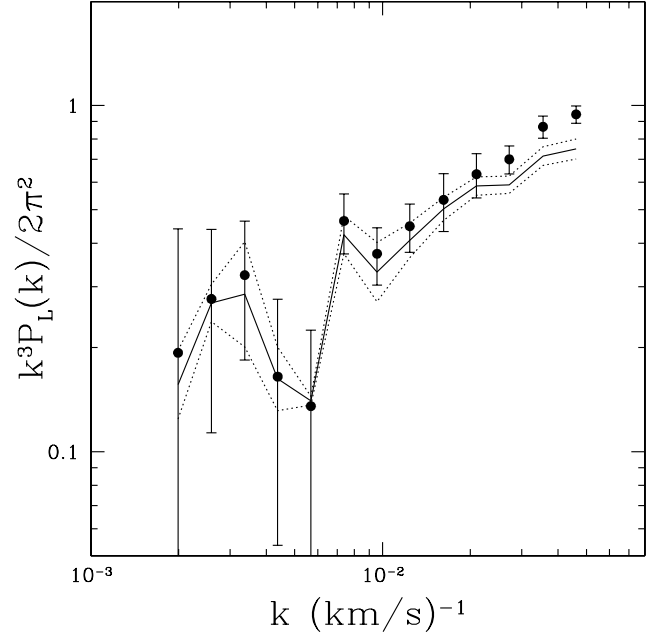


Figure 9. The "best fit" recovered linear power spectrum (solid line) and its 1-sigma systematic error bars (dotted lines).

Table 1. The recovered factored linear power spectrum  $P_L^{\text{fct}}$

$k$ (km/s) <sup>-1</sup>	$P_L^{\text{fct}}$ (km/s) <sup>3</sup>	Random err. (km/s) <sup>3</sup>	Systematic err. (km/s) <sup>3</sup>
1.99 10 <sup>3</sup>	3.92 10 <sup>6</sup>	5.02 10 <sup>6</sup>	0.90 10 <sup>6</sup>
2.59 10 <sup>3</sup>	3.06 10 <sup>6</sup>	1.80 10 <sup>6</sup>	0.38 10 <sup>6</sup>
3.37 10 <sup>3</sup>	1.47 10 <sup>6</sup>	0.63 10 <sup>6</sup>	0.53 10 <sup>6</sup>
4.37 10 <sup>3</sup>	3.85 10 <sup>7</sup>	2.59 10 <sup>7</sup>	0.82 10 <sup>7</sup>
5.68 10 <sup>3</sup>	1.51 10 <sup>7</sup>	1.00 10 <sup>7</sup>	0.44 10 <sup>7</sup>
7.38 10 <sup>3</sup>	2.08 10 <sup>7</sup>	0.41 10 <sup>7</sup>	0.26 10 <sup>7</sup>
9.58 10 <sup>3</sup>	7.42 10 <sup>6</sup>	1.40 10 <sup>6</sup>	1.46 10 <sup>6</sup>
1.24 10 <sup>2</sup>	4.23 10 <sup>6</sup>	0.67 10 <sup>6</sup>	0.49 10 <sup>6</sup>
1.62 10 <sup>2</sup>	2.34 10 <sup>6</sup>	0.43 10 <sup>6</sup>	0.18 10 <sup>6</sup>
2.10 10 <sup>2</sup>	1.25 10 <sup>6</sup>	0.18 10 <sup>6</sup>	0.08 10 <sup>6</sup>
2.72 10 <sup>2</sup>	5.79 10 <sup>6</sup>	0.54 10 <sup>6</sup>	0.33 10 <sup>6</sup>
3.55 10 <sup>2</sup>	3.15 10 <sup>6</sup>	0.23 10 <sup>6</sup>	0.20 10 <sup>6</sup>
4.61 10 <sup>2</sup>	1.51 10 <sup>6</sup>	0.09 10 <sup>6</sup>	0.10 10 <sup>6</sup>

quoted by us can be considered as an estimate for the systematic error in the Croft et al. (2001) measurement, but the precise value of such an error and its covariance matrix may depend very much on the specifics of the prior.

The observational data (Ricotti et al. 2000; Schaye et al. 2000; McDonald et al. 2001) sets the value of  $Q_{\text{T}}$  at

$$Q_{\text{T}} = 1 \pm 0.15 \quad (15)$$

and the error on  $Q_{\text{T}}$  is uncorrelated with the systematic error on  $P_L^{\text{fct}}(k)$ .

With the mean optical depth the story is more complicated, because there is no sufficiently accurate measurement of it. The PRS data give  $Q_{\text{PRS}} = 1.00^{+0.11}_{-0.08}$ , while the MCD data give  $Q_{\text{MCD}} = 1.18 \pm 0.07$ . Combining the two values in quadrature (because the data sets they used are independent), we find

$$Q_{\text{D}} = 1.11 \pm 0.05 \quad (16)$$

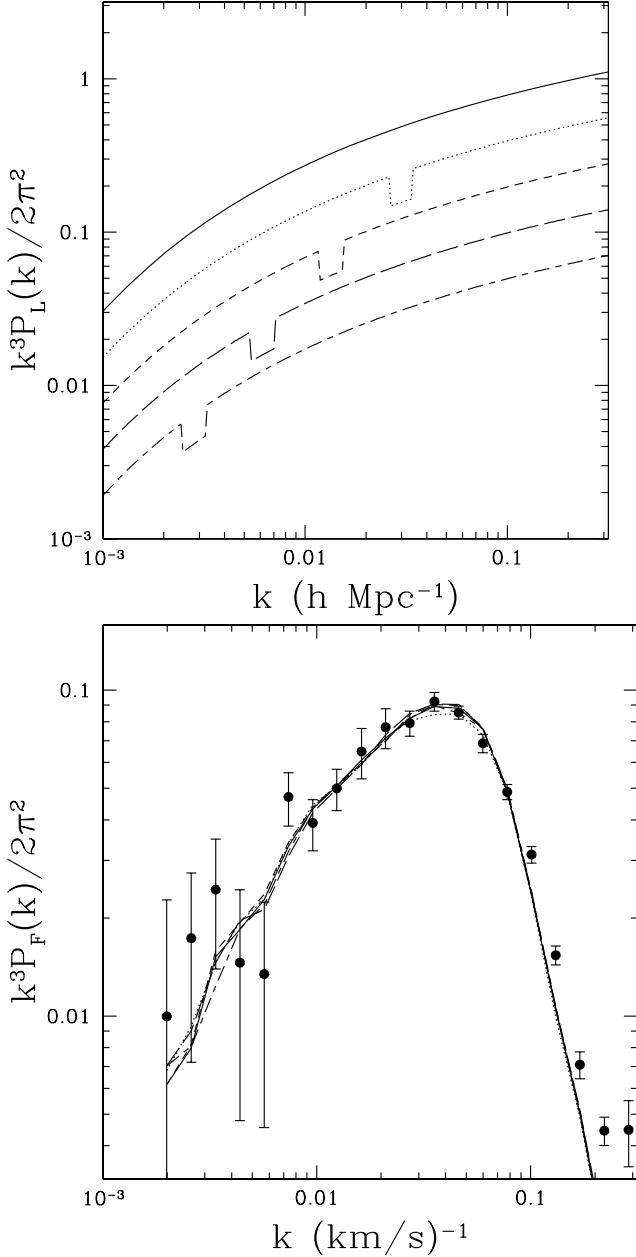


Figure 10. (a) The assumed prior linear power spectra for the fiducial Croft et al. model with the power reduced at a particular value of the wavenumber. The power spectra are offset vertically by 0.3 dex for clarity. (b) Their respective best-fit flux power spectra.

And for the most conservative estimate, we can include the whole range of quoted numbers:

$$0.9 < Q < 1.25: \quad (17)$$

### 3.2 Band-Power Windows

Measurements of flux power sample power not at a single wavenumber, but rather over a finite band of wavenumbers. The band power windows  $b(k; k^0)^2$  in equation (4) can be extracted by differentiating the flux power spectrum  $P_F(k)$  with respect to the linear power spectrum  $P_L(k)$ . The shape

of the band-powers emerges most clearly if they are scaled with the fiducial powers, so we define scaled band-power windows by

$$\frac{\partial \ln P_F(k)}{\partial \ln P_L(k^0)} = b^2(k; k^0) P_L(k) = P_F(k^0): \quad (18)$$

In order to measure the effective band-power windows in the present case, we ran four additional models with the fiducial power spectrum of Croft et al. (2001) reduced by 20% in four different wave-bands, corresponding to four  $k$  values. Linear power spectra for these models are shown in Figure 10a, and their respective flux power spectra are shown in Fig. 10b. The difference between the different models is comparable to the residual uncertainty in the mean flux power spectrum (Fig. 1), and thus we are only able to measure the difference between the various models with the reduced power to an accuracy of about 30%. A more accurate determination of the band-power windows would require an implausibly large number of simulations.

As can be seen, the abrupt reductions in the linear power spectrum lead not to abrupt reductions in the flux power spectrum, but rather to broad depressions. Figure 11 shows the inferred band-power windows themselves, the derivative of the flux power spectrum with respect to the input linear power spectrum at a given wavenumber, both for the case when the amplitudes of the input power spectra are kept fixed, and when the amplitudes are adjusted to fit the observed flux power spectrum. Evidently the effective band-power windows are quite broad.

Fig. 11 indicates that the band-power windows are broader at smaller scales. Figure 12 attempts to quantify this feature by showing the same derivatives as Fig. 11, except as a function of  $r = 2/k$  rather than  $k$ . To bring out the similarity of shapes, the four band-power windows from Fig. 11 have been shifted horizontally so that their center points  $r_0 = 2/k_0$  coincide (the centers of the band-power windows  $k_0$  do not necessarily fall on  $k^0$ , but are always within one bin in  $k$  space, from which we conclude that this discrepancy is most likely due to the finite  $k$ -space sampling), and vertically to the same maximum. The four band-power windows do not have exactly the same width in real space. Fitting to a Gaussian of width  $\sigma$ , we find that  $\sigma$  as a function of  $k^0$  can be approximated as

$$(k^0) \propto \frac{25 \text{ km/s}}{k^0 - 1 \text{ km/s}}: \quad (19)$$

In order to illustrate that it is indeed peculiar velocities that are responsible for the smoothing of the recovered linear power spectrum, we show in Fig. 12 the derivative of the flux power spectrum with respect to the prior linear power spectrum at  $k^0 = 0.0096 \text{ (km/s)}^{-1}$  (an equivalent of the long-dashed line) with all peculiar velocities set to zero. In this case the peak is much narrower, and its width is explained by finite sampling of the  $k$ -space alone.

It is important to underscore here that it is the power spectrum itself which is smoothed, and not the flux. Croft et al. (2001) did consider the effect of smoothing the Lyman-alpha absorption spectrum (Fig. 10 in their paper), but the effect that we discuss here is different – it is a correlation of power between the neighboring  $k$  values rather than a reduction in power on small scales.



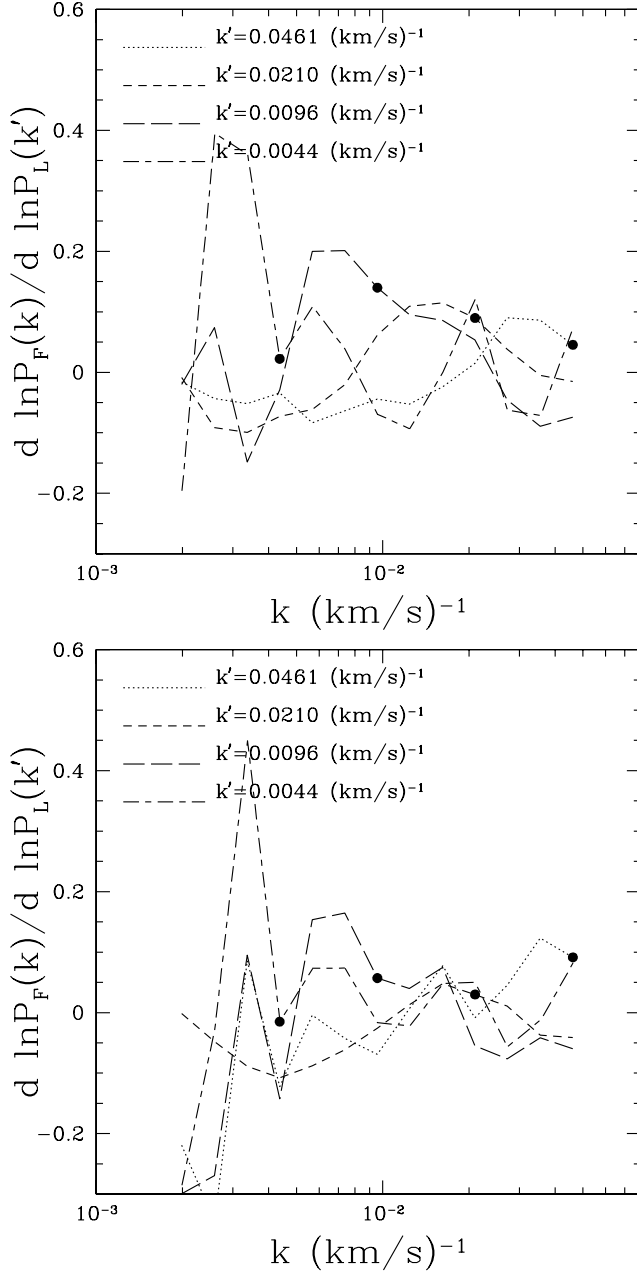


Figure 11. The derivative of the measured flux power spectrum with respect to the value of the input linear power spectrum at a given wavenumber for four wavenumbers, as labeled. The curves provide estimates of the effective band-power windows of the flux power spectrum. Filled circles show the values of  $k^0$ . Two cases are shown: (a) the amplitudes of the input power spectra are fixed to  $z = 2.72$  ( $\Omega_b = 0.23$ ) and (b) the amplitudes of the input linear power spectra are adjusted to achieve the best fit to the observed flux power spectrum.

This effect is easy to understand physically. Let us imagine that the matter power spectrum is a delta function, i.e. the power is only nonzero at a given value  $k_0$ . In the absence of peculiar velocities the three-dimensional flux power spectrum would be non-zero only in a narrow range of scales around  $k_0$  (we cannot claim that this range is infinitesimally small because the relationship between the linear matter

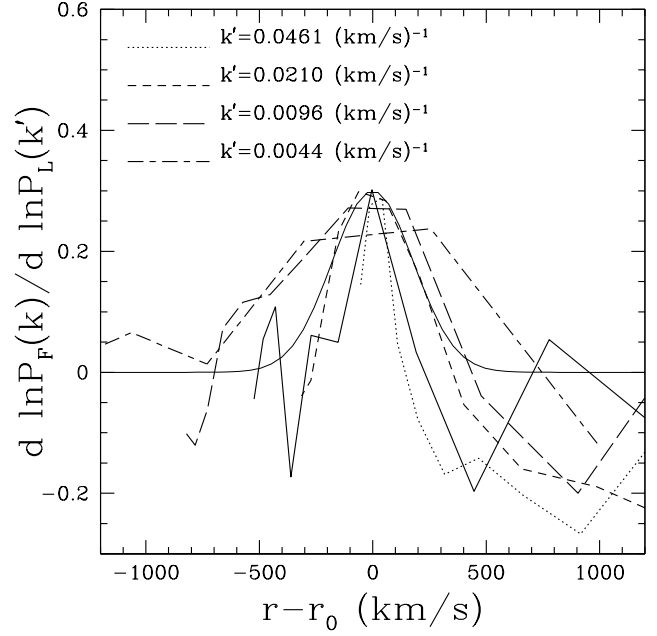


Figure 12. The derivative of the measured flux power spectrum with respect to the value of the input linear power spectrum at a given wavenumber for four wavenumbers and for the fixed amplitude of the prior power spectra shown as a function of  $r - r_0$ , where  $r = 2/k$ . This is essentially Fig. 11 with a transformed x-axis. The bold solid line shows what the long-dashed line becomes when peculiar velocities are set to zero. The curves are scaled vertically to have the same amplitude at maximum. The thin solid line shows a Gaussian with  $\sigma = 200$  km/s, which is a fit to the short-dashed line.

power spectrum and the Lyman-alpha flux power spectrum is nonlinear; however, the solid line in Fig. 12 does demonstrate that this range is less than the  $k$ -space sampling in Croft et al.). In the presence of peculiar velocities a given structure in physical space would appear shifted along the line of sight in redshift space (which is where the flux is measured), thus smearing power over a range of scales comparable to the 1D velocity dispersion.

### 3.3 Missing physics

In the previous subsections we have considered only one possible source of the systematic error, namely the choice of the prior linear power spectrum. Another possible uncertainty comes from the fact that no simulation includes all of the relevant physics. We can identify at least three major physical ingredients that are missed by pure PM simulations:

- (i) gas pressure;
- (ii) inhomogeneities in the ionizing background;
- (iii) shocks in the gas.

We discuss these effects in that order.

#### 3.3.1 Gas pressure

The role of gas pressure is well understood. In the linear regime it can simply be expressed by the filtering scale of baryonic perturbations,  $k_F$ :

$$P_{\text{gas}}(k) = P_{\text{DM}}(k) e^{2k^2=k_F^2}; \quad (20)$$

where  $k_F$  is a complicated function of the entire thermal history of the universe (Gnedin & Hui 1998), and equation (20) is a good approximation to the exact solution to the linear theory equations for  $k < 0.8k_F$ . There are also strong reasons to believe that the filtering scale describes the effect of gas pressure even in the nonlinear regime (Gnedin 2000b).

Recent measurements of the thermal history of the universe (Ricotti et al. 2000; Schaye et al. 2000; McDonald et al. 2001) give  $k_F = (35 \pm 5) h \text{ Mpc}^{-1}$ , significantly smaller than the range of scales  $k < 3 h \text{ Mpc}^{-1}$  measured from the Lyman-alpha forest power spectrum (the reason being that pressure filtering, always lagging behind the growth of the Jeans mass, is subdominant to the thermal broadening of the absorption spectrum). Thus, the pressure filtering produces only about 2% correction to the recovered linear power spectrum, and it is unmeasurable at the current time. This is, of course, in a full agreement with the conclusions of Croft et al. (2001).

### 3.3.2 Inhomogeneities in the ionizing background

Inhomogeneities in the ionizing background can come from two classes of sources: large scale inhomogeneities from quasars, and small scale inhomogeneities from galaxies. The former is known to be unimportant (Croft et al. 1999), but the effect of the latter can only be estimated from advanced numerical simulations which include effects of the radiative transfer. Here we use a simulation from Gnedin (2000a). We follow the Croft et al. (2001) procedure for the last output of this simulation at  $z = 4$ , but we analyze it two different ways. In the first case we use the neutral hydrogen fraction from the simulation data (which reflects the non-uniformity of the ionizing radiation background) to compute a synthetic Lyman-alpha forest at  $z = 4$ . In the second case we assume that the ionizing radiation is uniform and compute the neutral hydrogen fraction from ionization equilibrium. The value of the background is calculated by normalizing to the mean opacity in the simulation, so that in both cases the mean opacity is the same. In both cases we adopt the gas temperature as given in the simulation. After computing the flux power spectra in both cases, we find that they differ by less than 1%.

The Gnedin (2000a) simulation suffers from its small box size ( $4 h^{-1} \text{ Mpc}$ ), and therefore a 1% difference is probably an underestimate, but it appears unlikely that it underestimates the role of inhomogeneities in the ionizing background by, say, a factor of 10. We therefore conclude that inhomogeneities in the ionizing background do not bias the measurement of the matter power spectrum from the Lyman-alpha forest.

Surprisingly, while the power spectra in the two calculations are very similar, the actual value of the volume averaged photoionization rate differs by 20%, being larger for the inhomogeneous ionizing background. Thus, simulations that assume homogeneous ionization and adjust the photoionization rate to fit the mean opacity of the forest actually underestimate the photoionization rate by at least 20%, or, equivalently, overestimate the baryon density by at least 10% (and probably by a significantly larger factor).

This may explain larger numbers for the baryon density typically found in such simulations (Haehnelt et al. 2001).

One of the possible concerns with this conclusion is that the Gnedin (2000a) simulation was terminated at  $z = 4$ , whereas the Croft et al. (2001) measure the linear matter power spectrum at  $z = 3$ .

However, observationally we know that the following three quantities do not change by more than a factor of two between  $z = 4$  and  $z = 3$ : the mean photoionization rate (Lu et al. 1996; Cooke et al. 1997; Scott et al. 2000), the star formation rate (Steidel et al. 1999), and the mean separation between star forming galaxies (deduced from constancy of the mean UV luminosity density and the star formation rate). This immediately implies that the proximity regions of star forming galaxies occupy approximately the same fraction of the total volume at  $z = 4$  and  $z = 3$ , and thus expected fluctuations in the ionizing background are comparable at  $z = 4$  and  $z = 3$ . We thus can be confident that our conclusions about the role of fluctuations in the ionizing background at  $z = 4$  also hold at  $z = 3$ .

### 3.3.3 Shocks and other mess

Obviously, non-gravitational effects like shocks can significantly affect the distribution of the Lyman-alpha forest. Fortunately, we have observational data (Ricotti et al. 2000; Schaye et al. 2000; McDonald et al. 2001) that suggest that non-gravitational effects are not significant in the forest. First, the IGM temperature at  $z = 3$  is quite low, only 20,000 K, and is entirely consistent with pure photoheating of the gas. Second, the narrowness of the cut-off in the Doppler parameter vs column density distribution of the Lyman-alpha lines suggests that the photoionization-induced "effective equation of state" has a small scatter, again fully consistent with the pure photoheating of the gas. Any realistic shock heating would destroy this tight correlation.

Thus, while we cannot rigorously prove that shocks and other non-gravitational effects can be neglected in modeling the Lyman-alpha forest, they would require a rather special fine-tuning which closely mimics the work of gravity and photoionization.

## 4 CONCLUSIONS

The two main drawbacks of the Croft et al. (2001) paper are (a) that it misses the dependence of the recovered linear power spectrum on cosmological parameters (eq. [13]) and (b) that it misses the fact that the effective band-power windows of the flux power spectrum are broad. The broad band-powers must induce broad correlations between estimates of the flux power, and consequently also of the recovered matter power spectrum. But as the whole, we must acknowledge that the measurement that they present is remarkable: it currently offers the best measurement of the linear matter power spectrum over a range of scales that are nonlinear today.

The effective band-power windows can be approximated as Gaussians with a dispersion  $k = k^{3=2} = (2 \pm 25 \text{ (km/s)}^{1=2})$  in Fourier space:

$$P_L^{\text{REC}}(k) = \frac{1}{k^2} \int_0^1 dk^0 P_L^{\text{TRUE}}(k^0) e^{-\frac{(k-k^0)^2}{2k^2}}; \quad (21)$$

where  $P_L^{\text{REC}}(k)$  is the recovered and  $P_L^{\text{TRUE}}(k)$  is the true underlying linear power spectra respectively. The smoothing is caused by peculiar velocities.

And while the resulting strong covariance between estimates of power at different wavenumbers will make careful comparison of the data and cosmological models more complicated than simple fitting, this measurement will undoubtedly play an important role in securing accurate values of the cosmological parameters.

We also notice in passing that residual inhomogeneities in the ionizing background do not affect the measurement of the linear power spectrum, but may substantially bias estimates of the cosmic baryon density from the Lyman-alpha forest data.

We thank Rupert Croft and David Weinberg for valuable comments. We are also grateful to Rupert for providing the revised version of their paper prior to posting it to astro-ph. This work was partially supported by NASA ATP grant NAG 5-10763 and by the National Computational Science Alliance under grant AST-960015N, and utilized the SGI/CRAY Origin 2000 array at the National Center for Supercomputing Applications (NCSA).

## REFERENCES

- Cooke, A. J., Espey, B., Carswell, B. 1997, *MNRAS*, 284, 552  
 Croft, R. A. C., Weinberg, D. H., Pettini, M., Hemquist, L., Katz, N. 1999, *ApJ*, 520, 1  
 Croft, R. A. C., Weinberg, D. H., Bolte, M., Burles, S., Hemquist, L., Katz, N., Kirkman, D., Tytler, D. 2001, *ApJ*, in press (astro-ph/0012324)  
 Ferrell, R., Bertschinger, E. 1994, *Int. J. Mod. Phys.*, C5, 933  
 Gnedin, N. Y. 2000a, *ApJ*, 535, 530  
 Gnedin, N. Y. 2000b, *ApJ*, 542, 535  
 Gnedin, N. Y., Hui, L. 1998, *MNRAS*, 296, 44  
 Gunn, J. E., Peterson, B. A. 1965, *ApJ*, 142, 1633  
 Haehnelt, M. G., Madau, P., Kudritzki, R., Haardt, F. 2001, *ApJ*, 549, L1  
 Hui, L., Gnedin, N. Y. 1998, *MNRAS*, 292, 27  
 Hui, L., Gnedin, N. Y., Zhang, Y. 1997, *ApJ*, 486, 599  
 Lu, L., Sargent, W. L. W., Omble, D. S., Takada-Hidai, M. 1996, *ApJ*, 472, 509  
 McDonald, P., Miralda-Escude, J., Rauch, M., Sargent, W., Barlow, T., Cen, R., Ostriker, J. P. 2000, *ApJ*, 543, 1  
 McDonald, P., Miralda-Escude, J., Rauch, M., Sargent, W., Barlow, T., & Cen, R. 2001, *ApJ*, submitted (astro-ph/0005553)  
 Press, W. H., Rybicki, G. B., Schneider, D. P. 1993, *ApJ*, 414, 64 (PRS)  
 Ricotti, M., Gnedin, N. Y., Shull, J. M. 2000, *ApJ*, 534, 41  
 Schaye, J., Theuns, T., Rauch, M., Efstathiou, G., Sargent, W. L. W. 2000, *MNRAS*, 318, 817  
 Scott, J., Bechtold, J., Dobrzycki, A., Kulkarni, V. P. 2000, *ApJ*, 130, 67  
 Steidel, C. C., Adelberger, K. L., Cavaletto, M., Dickinson, M., Pettini, M. 1999, *ApJ*, 519, 1